Science of the Total Environment 544 (2016) 995–1007

Contents lists available at ScienceDirect

Science of the Total Environment

journal homepage: www.elsevier.com/locate/scitotenv

Marine water from mid-Holocene sea level highstand trapped in a coastal aquifer: Evidence from groundwater isotopes, and environmental significance

Stephen Lee [a], Matthew Currell [a,*], Dioni I. Cendón [b,c]

[a] School of Civil, Environmental and Chemical Engineering, RMIT University, Melbourne, Australia [b] Australian Nuclear Science and Technology Organisation, Kirrawee, Australia [c] Connected Water Initiative, School of Biological, Earth and Environmental Sciences, University of New South Wales (UNSW), Sydney, Australia

HIGHLIGHTS

- Stable and radiogenic isotopes used to assess age and sources of saline groundwater
- Radiocarbon ages indicate midHolocene emplacement during high sea-stand.
- Stable isotopes indicate marine and fresh water mixing subject to transpiration.
- Vertical salinity profiles and $\delta^{13}C$ indicate emplacement by surface inundation.
- C-isotope mass balance points to extensive groundwater-mangrove interaction

article info

Article history:
Received 28 October 2015
Received in revised form 3 December 2015
Accepted 3 December 2015
Available online 17 December 2015

Editor: D. Barcelo

Keywords:
Coastal aquifer
Groundwater salinity
Holocene
Trapped seawater
Sea level
Isotopes

GRAPHICAL ABSTRACT

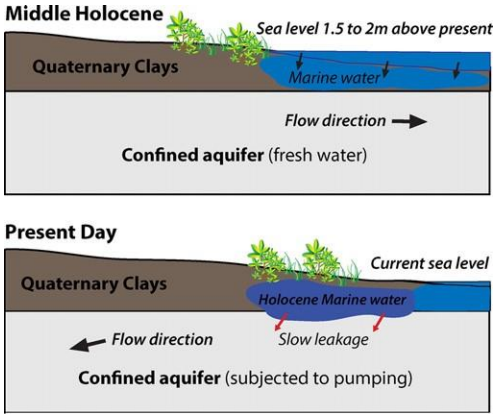

a b s t r a c t

A multi-layered coastal aquifer in southeast Australia was assessed using environmental isotopes, to identify the origins of salinity and its links to palaeo-environmental setting. Spatial distribution of groundwater salinity (electrical conductivity values ranging from 0.395 to 56.1 mS/cm) was examined along the coastline along with geological, isotopic and chemical data. This allowed assessment of different salinity sources and emplacement mechanisms. Molar chloride/bromide ratios range from 619 to 1070 (621 to 705 in samples with EC N15 mS/cm), indicating salts are predominantly marine. Two distinct vertical salinity profiles were observed, one with increasing salinity with depth and another with saline shallow water overlying fresh groundwater. The saline shallow groundwater (EC = 45.4 to 55.7 mS/cm) has somewhat marine-like stable isotope ratios ($\delta^{18}O$ = −2.4 to −1.9 ‰) and radiocarbon activities indicative of middle Holocene emplacement (47.4 to 60.4 pMC). This overlies fresher groundwater with late Pleistocene radiocarbon ages and meteoric stable isotopes ($\delta^{18}O$ = −5.5 to −4.6‰). The configuration suggests surface inundation of the upper sediments by marine water during the mid-Holocene (c. 2–8 kyr BP), when sea level was 1–2 m above today's level. Profiles of chloride, stable isotopes, and radiocarbon indicate mixing between this pre-modern marine water and fresh meteoric groundwater to varying degrees around the coastline. Mixing calculations using chloride and stable isotopes show that in addition to fresh-marine water mixing, some salinity is derived from transpiration by halophytic vegetation (e.g. mangroves). The $\delta^{13}C$ ratios in saline water (−17.6 to −18.4‰) also have vegetation/organic matter signatures, consistent with emplacement by surface inundation and extensive interaction between vegetation and recharging groundwater. Saline shallow groundwater is preserved only in areas where low permeability sediments have slowed subsequent downwards propagation. The configuration is unlikely to be stable long-term due to fluid density; this may be exacerbated by pumping the underlying aquifer.

∗ Corresponding author at: GPO Box 2476, Melbourne, VIC 3000, Australia. E-mail address: Matthew.currell@rmit.edu.au (M. Currell).

http://dx.doi.org/10.1016/j.scitotenv.2015.12.014 0048-9697/

1. Introduction

Coastal aquifers are some of the most important water sources globally, and pressure on these aquifers is expected to intensify in the coming decades (Ferguson and Gleeson, 2012). In all coastal aquifers, a zone of mixing occurs between fresh groundwater and marine water, which form an interface. The shape and properties of this interface are controlled by a range of factors, including sea-levels, groundwater hydraulic heads and flow velocities, geological structure, and the variable density properties of the two fluids. In steady state systems or those in which equilibrium is reached rapidly between sea level and aquifer hydraulic heads, this interface can be easily predicted with analytical or numerical modeling (e.g. Werner et al., 2013). However, coastal environments are by nature highly dynamic, being subjected to continual geomorphological and hydrological evolution due to sea level change, climate change and variable sedimentation and erosion rates. These factors may cause disequilibrium between the position of the salt-fresh water interface and current sea levels (e.g. Kooi and Groen, 2003; Morrissey et al., 2010).

The influence of palaeoclimatic and geomorphological processes on salt-fresh water interfaces in coastal aquifers is evident in the global occurrence of 'vast meteoric groundwater reserves' (VMGRs) in offshore areas (Post et al., 2013). These large bodies of offshore fresh or brackish groundwater show that many coastal groundwater systems are out of equilibrium with current sea levels, and that palaeoenvironmental conditions of the Late Pleistocene and Holocene still influence the interface position. VMGRs exist due to prior activity of fresh groundwater systems in areas now below ocean, yet to be displaced by marine water. Less well documented is the occurrence of saline water bodies of marine origin in continental groundwater systems, emplaced during periods of higher sea level than the present

e.g., 'seawater emplaced during the Quaternary' (SEDQ). While likely to be much more localised in time and space than VMGRs, due to the current sea level position being relatively high by recent geological standards, there are examples of low lying areas where inundation by seawater in previous times (e.g. the mid-Holocene) appears evident (Giambastiani et al., 2012; Vaeret et al., 2012; Currell et al., 2014; Cary et al., 2015). Key controls on the presence of such trapped marine water in coastal aquifers are changes in relative coastline elevation due to sea level change, evolution of the aquifer water balance, and the geological structure and aquifer properties, which control the rate of re-equilibration of the interface following a sea level change (Kooi et al., 2000).

In this study, we examine a coastal aquifer system which has been subject to complex geological, geo-morphological and hydrological evolution, and use a range of physical and chemical indicators to determine the origins of groundwater salinity, and its relationship to the palaeoenvironment. The area has previously been the subject of detailed hydrogeological assessments (e.g. Jenkin, 1962; Lakey and Tickell, 1980; Cheng, 1998) as it is an important water supply aquifer considered vulnerable to salinization, due to its low lying position at the coast. However it has to date been assumed that the aquifer system responds rapidly to changes in water balance and sea level, and so the impact of past processes (e.g. during the late Pleistocene and Holocene) has generally been ignored in the interpretation of groundwater salinity data. Understanding the origins of salinity and constraining the timescales of salinization (and freshening) is vitally important for future management of this and other similar coastal aquifer systems worldwide. For example, aquifers with groundwater salinity resulting from past transgression/inundation events in geological time may require different protection strategies to aquifers experiencing 'classic' seawater intrusion.

2. Background and setting

Western Port Bay, located approximately 40 km South-East of Melbourne, Australia (Fig. 1) is a shallow marine embayment, with maximum seafloor depth of approximately 30 m. The area is characterised by mudflats, drained swampland and an extensive tidal channel system (Marsden et al., 1979; Table 1). Below and inland of the bay is a multilayered sedimentary basin — the Western Port Basin, filled with coastal sediments and volcanic deposits ranging from Palaeocene to Holocene age (Carrillo-Rivera, 1975). These form important aquifers containing fresh water used for irrigation in the Koo Wee Rup Water Supply Protection Area. The Western Port Basin is bordered by the Great Dividing Range to the north, the South Gippsland Highlands in the east, and the Mornington Peninsula to the west (Fig. 1). It has been subject to block faulting and periodic marine transgression and regression throughout the Cainozoic (Table 1). Major periods of sedimentary and volcanic deposition occurred with subsidence along basin faults (Heath Hill and Tyabb Faults), which form the eastern and western margins (SpencerJones et al., 1975).

2.1. Sea levels and coastal history

Western Port Bay would have been periodically inundated and emptied of seawater over the Quaternary period as sea levels rose and fell. For example, the bay would have been cut off from the ocean throughout much of the most recent glacial period, when sea level was approximately 125 m below present (Lewis et al., 2013) (Fig. 2). The land surrounding the bay is low elevation and flat (e.g., between 1 and 5 m above current mean sea level up to a distance of ~10 km in-land), and much of the area was swampland before draining and clearing for agriculture occurred in the 19th century. The sea level rise event following the end of the last glacial maximum (LGM) would have inundated a large area previously sitting ~100 m above sea level (Fig. 2), prompting a rise in groundwater base level (Kafri and Yechieli, 2010), the landwards progradation of pre-existing surface and ground water systems, and encouraging the (re-)formation of swamplands across the lowlying Western Port plains (Marsden and Mallett, 1975). Sea levels reached their maximum during the Holocene, between ca. 2 and 8 thousand years (kyr) before present throughout southern Australia (Sloss et al., 2007; Lewis et al., 2013). At this time relative sea-level is estimated to have been 1.5–2 m above the present high water mark at Western Port, on the basis of geomorphological evidence, including stranded cliff lines, barrier dunes and marine shell-beds inland of the present coast (Marsden and Mallett, 1975; Table 1). This evidence indicates that extensive areas around the current coastline were periodically to permanently inundated with marine water in the Holocene palaeo-swampland. Western Port is characterised by a wide mangrove fringe at the coast and scattered patches of swamp paper bark vegetation — remnants of the larger old swamp, amongst predominantly agricultural land. Vegetation within the submerged tidal channel and mudflats is dominated by seagrass beds, including Zostera muelleri and other species.

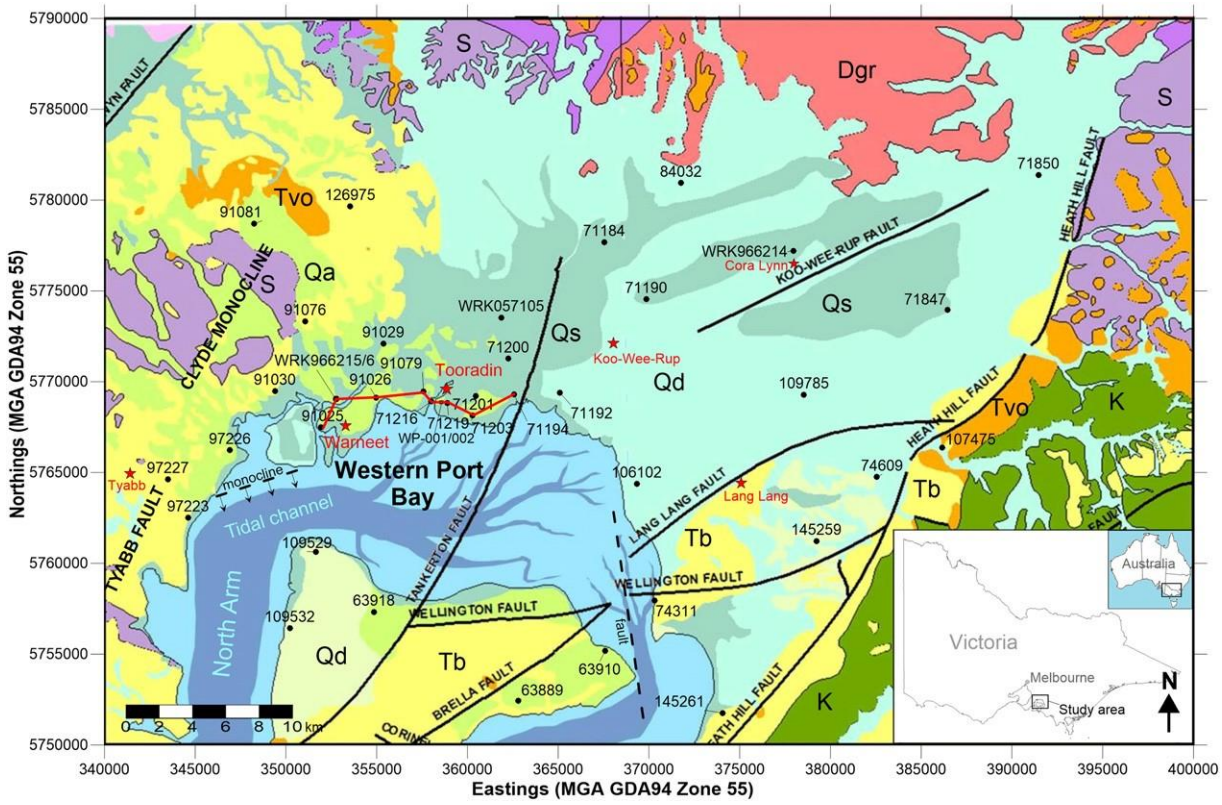

Fig. 1. Surface geological map of the Western Port Basin, showing location of sampled monitoring wells. Surface geological units: Qa (Quaternary aeolian); Qs (Quaternary swamp); Qd (Quaternary alluvial deposits); Tb (Baxter Formation); Tvo (Older Volcanics); K (Strzelecki Group mudstones); Dgr (Devonian granite); S (Silurian mudstone). The line of section for Fig. 4 is shown in red.

2.2. Geology and hydrogeology

The upper geological layer of the onshore Western Port Basin consists mainly of clay-rich Quaternary swamp deposits. These act as an effective aquitard covering much of the Basin (to a maximum thickness of ~60 m), although the clays thin and are not continuous in all areas. The Quaternary clays are generally absent near Warneet, the Tyabb coast, and in the main tidal channel (north arm) of Western Port Bay. Below the Quaternary swamp deposits, the geology comprises a set of interlayered aquifers with varying extents of confinement and interconnectivity. These freshwater bearing units consist of Cainozoic sediments and volcanic rocks deposited into a subsiding graben, above Silurian, Devonian, or Mesozoic bedrock (Lakey and Tickell, 1980). The main aquifers from which fresh groundwater is extracted are the confined Western Port Group sediments, consisting of the Baxter Formation (terrestrial sands, gravels, clays and lignite), Sherwood Formation (marine limestone, mud and silt), Yallock Formation (terrestrial gravel, clay and silt); and the Older Volcanics (highly weathered and fractured basalt). Currell et al. (2013) present a more detailed stratigraphy of the basin and discussion of these aquifers. Areas in the vicinity of the main faults, where the aquifer units are at or close to the surface, are believed to be major recharge areas for the confined aquifer system (Currell et al., 2013).

Within Western Port Bay, two major islands exist, Philip Island located to the South of the study area, and French Island, a basement high formed by block faulting, in the centre (Fig. 1). In the bay, the tidal channel is incised into seafloor clays and sands, bringing the seabed to depths of up to 30 m, and exposing the Western Port Group to potential seawater interaction. This exposed patch of aquifer is believed to be a submarine groundwater discharge and/or seawater recharge zone (Lakey and Tickell, 1980). Before intensive groundwater development, groundwater flowed out towards the bay, discharging into the tidal channel through fine silt and sand outcrops of the Western Port Group (Baker et al., 1986).

2.3. Groundwater chemistry

The chemistry of groundwater in Western Port Basin was reported by Jenkin (1962), Thompson (1974), Carrillo-Rivera (1975)), Cheng (1998) and Currell et al. (2013). Groundwater major ions are mostly dominated by sodium and chloride, with locally elevated calcium, magnesium and bicarbonate contents associated with carbonate minerals in the marine Sherwood Formation (Currell et al., 2013). Groundwater ranges from oxygen-rich to reducing, and methanogenesis linked to sulfate reduction is locally observed in organic-rich parts of the aquifer (Lee, 2015).

The origins of salinity, controls on its spatial distribution and change in salinity over time have not yet been assessed in detail in the Western Port Basin using isotopic evidence. Saline water was discovered in the north-west corner of French Island in an investigation by Jenkin (1962). A hydrogeological investigation by Carrillo-Rivera (1975) speculated that groundwater with seawater-like composition near the coast at Warneet was emplaced at the time of geological deposition (i.e. connate water). Recently, Currell et al. (2013) showed that groundwater in the central and coastal parts of the Western Port Basin is thousands to tens of thousands of years old (radiocarbon activities ranging from 1.0 to 24.9 pMC), which suggests recharge predominantly during the late Pleistocene, and rules out incomplete flushing of waters trapped at the time of sediment deposition. Lakey and Tickell (1980) proposed that highly saline groundwater near the coast is the result of saltwater intrusion

due to over-pumping of the aquifers, causing leakage into the tidal channel and horizontal movement towards the pumping area. However, their study did not evaluate the age of salinization and assumed relatively short timescales for migration of saline water.

Table 1
Relative sea level and geological/geomorphological activity in the Western Port Basin during the Quaternary. Modified from Marsden and Mallett (1975).

Era/time (years BP)	Relative sea level	Geological/geomorphological activity
	Small-scale/local changes	Present-day fluvial/coastal modifications. Swamp drainage for agriculture.
	Present day level	Progradation of intertidal zones.
	Regressive phase	Abandonment of depositional and erosional features of high sea-level.
Holocene (Est. 2000 to 8000)	Maximum: 1 to 2 m above present day level	Start of rapid progradation of barriers, beach systems.
	Flandrian Transgression	Swamp development. Drowning of relic topography and sediments; drainage disruption. Increase in sediments derived from Mesozoic source material
Late Pleistocene 16,000	Rising	Start of marine re-working of sediment. Some net nward movement, including to intertidal zone. d resent day marine cycle in Western Port
Start of post-Glacial sea level rise an Bay		
18,000 to 20,000 Pleistocene (Kosciusko Glaciation)	Low; ~125 m below present	Erosion: sediment transported beyond present shore. Aeolian activity. Minor tectonic movement – Bass, Almurta Faults.
Pleistocene Last Interglacial (or earlier) 125,000	High	Extensive fluvial deposition (limits beyond present shore). Cainozoic sediments (upthrown areas) important sediment source.
Early Pleistocene	Low	Main fault movements. Start of erosion — stripping, and sediment transport to beyond present shore. Establishment of major drainage systems.

2.4. Groundwater pumping and management

Following draining of swampland, groundwater development for irrigated agriculture in the Western Port Basin began in the first half of the 20th century, and grew rapidly until the 1960s. At this time, two large cones of depression formed in the confined aquifer below the main irrigation areas (Lakey and Tickell, 1980; Baker et al., 1986). In particular areas, including at the coast, groundwater levels periodically declined up to 5 m below sea level in response to pumping. At this time, there is anecdotal evidence that some irrigation bores began to be affected by salinization. However, the extent of salinization, or its mechanism was not well understood. Management of groundwater commenced in the early 1970s, involving licensing of production wells and determining caps on extraction. Although groundwater levels now recover seasonally after the main period of groundwater pumping each year, a cone of depression persists in the main agricultural areas during peak use periods (generally November to March) and these can extend into the bay in years of high abstraction, raising the risk of potential saline intrusion. At present, there is an overall cap set on groundwater abstraction of 1.28×10^7 m^3 per year, of which approximately 50 to 75% is typically used, depending on yearly climate. The basin has been divided into zones, and no additional usage above current levels is permitted in zones considered most vulnerable to saline intrusion (near the coastline). Water users can apply to trade their allocated water out of, but not into these districts (Southern Rural Water, 2010).

3. Materials & methods

3.1. Field sampling and lab analysis procedures

Groundwater sampling was conducted using monitoring wells in the Victorian State Observation Bore Network, while two additional new wells (WP-001 and WP-002) owned by Melbourne Water Corporation were also utilised. Monitoring wells located along the coastline sampling a range of depths and aquifer units were targeted, in order to develop a detailed picture of the saltwater and freshwater

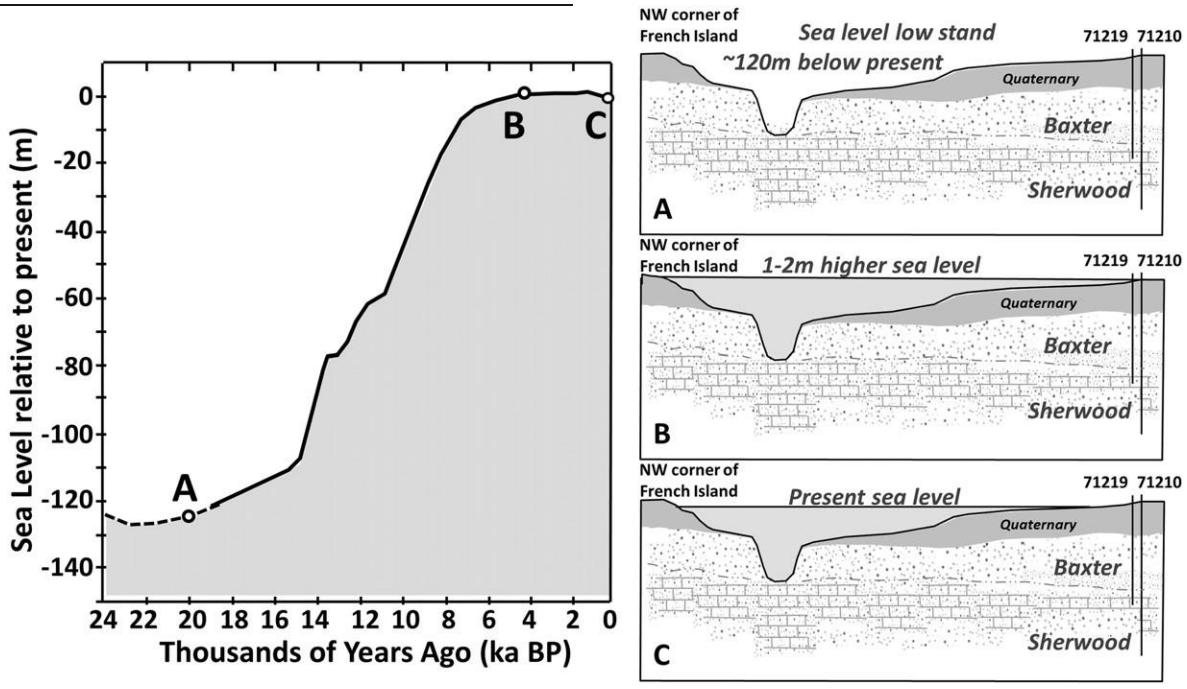

Fig. 2. Historical sea level change and likely relationship to coastline at Western Port (based on a topographic section between Tooradin and the northwest corner of French Island). A) c.20 kyr BP, tidal channel fully exposed; B) c.2–8 kyr BP, sea level maximum (1-2 m above current sea level) causes inundation of low-lying coastal areas; C) present day sea level. Number codes 71219 and 71210 are monitoring bores at Tooradin.

distribution. Most wells are constructed from 100 mm internal diameter PVC with slotted screens; one open borehole (91025) was also sampled. Past data collected from the monitoring network assisted with identification of zones of saline and fresh groundwater for selective isotopic sampling.

Groundwater samples were collected following procedures outlined in Currell et al. (2013), using pumps including: 1) 12-volt submersible pump (Proactive Supertwister), 2) Piston Pump (Bennett) and 3) Double Valve Pump (Solinst). In the field, physico-chemical parameters including electrical conductivity (EC), temperature, pH, and dissolved oxygen (DO) were monitored using a HACH HQ40d or YSI 556 handheld water quality meter, and stabilisation of parameters, as well as water levels, was achieved prior to sampling. Samples were filtered through 0.45 μm filter paper or in-line filters (AquaporeTM) and collected in HDPE bottles filled to the top and capped, minimising atmospheric contact, then refrigerated at 4 degrees Celsius until analysis. Alkalinity titrations were performed in the field with a HACH digital titrator, using 0.16 N/1.60 N Sulfuric acid and Bromocresol Green/Methyl Red indicator. Samples for cation analysis were acidified in the field with concentrated analytical grade HNO_3.

Major anions were analyzed at Monash University's School of Earth, Atmosphere and Environment using an Ion Chromatograph and ICP-MS for major cations, in both cases following methods described in Cartwright et al. (2010). Stable isotopes of water were analyzed at the Monash University School of Earth, Atmosphere and Environment, using a Finnigan MAT 252 Isotope Ratio Mass Spectrometer (IRMS), or the Australian Nuclear Science and Technology Organisation (ANSTO) using a Delta V Advantage IRMS, following methods in Cendón et al. (2014). At Monash University, $\delta^{18}O$ were measured by equilibrating with a He-CO_2 gas mixture for between 24 to 48 h at 32 °C in a ThermoFinnigan Gas Bench using continuous flow. Deuterium ratios (δ^2H) were measured using a Finnigan MAT H-Device by reduction with Cr at a temperature of 850 °C. Results are reported against VSMOW using delta (δ) notation, and are accurate to 1‰ for δ^2H and 0.2‰ for $\delta^{18}O$. $\delta^{13}C$ values were determined using IRMS at Monash University, following methods outlined in Currell et al. (2013).

Samples for tritium were distilled and electrolytically enriched prior to being analyzed by liquid scintillation spectrometry at the National Isotope Centre, New Zealand (Morgenstern and Taylor, 2009), or at ANSTO. ^3H concentrations are expressed in tritium units (TU), and have an approximate detection limit of 0.025TU. Samples from ANSTO have 1σ uncertainties between 0.02 and 0.03, with a minimum quantification limit of 0.05TU.

Radiocarbon analysis of groundwater was conducted at ANSTO. Measurement of radiocarbon activities was done on graphite targets by accelerator mass spectrometry, using the ANSTO 2MV tandetron accelerator STAR (Fink et al., 2004). The results are reported as percent Modern Carbon (pMC), with a range of 1σ errors between 0.03 and 0.4. Calculation of ^{14}C ages as uncorrected ages in calendar years before present were performed according to methods in Stuiver and Polach (1977).

3.2. Radiocarbon age corrections

The computer program NETPATH (Plummer et al., 1994) was used to correct groundwater ages from raw to corrected age estimates based on analysis of stable isotopes of carbon ($\delta^{13}C$), major ion chemistry, pH and alkalinity, and analysis of water sources and flow paths. The revised Fontes and Garnier model, as described in Han and Plummer (2013), was predominantly used to correct the ages and estimate residence times. Processes that were accounted for that are known to impact the overall dissolved inorganic carbon (DIC) pool include carbonate dissolution and old organic matter input (e.g. from lignite or peat in the aquifer), which were assumed to have $\delta^{13}C$ values of 0 and −25.0‰ respectively, and a^{14}C values of 0 pMC. Because it is acknowledged that correction of radiocarbon ages to 'true' groundwater ages is highly uncertain in most geological systems (including the current study) a range of model assumptions were used, and estimates of groundwater age are reported as minimum and maximum (uncorrected) ages, based on the output of multiple model runs. Further detail is included in Lee (2015).

3.3. Mixing calculations

Proportions of seawater and fresh meteoric water in groundwater were estimated according to mass balance in a two end-member system, using two independent indicators — chloride and $\delta^{18}O$ (Eqs. (1) & (2), respectively): $m_{Clsample}$ $m_{Clfresh}$

f 1

sea ¼ ð Þ

m_{Cl} $m_{Clfresh}$

$\delta_{18}O$ δ_{18}

$f_{sea} = \frac{\delta^{18}O_{sample} - \delta^{18}O_{fresh}}{\delta^{18}O_{sea} - \delta^{18}O_{fresh}}$ (2)

The factor f_{sea} represents the fraction (between 0 and 1) of marine water estimated in a groundwater sample of mixed origin, with the residual assumed to comprise fresh groundwater of meteoric origin. The end-members used for seawater were chosen using average values of $\delta^{18}O$ and Cl for Western Port Bay seawater (n = 4), while for fresh water the end-member used average rainfall chloride for Melbourne of 0.15 mmol/L and the average $\delta^{18}O$ of fresh groundwater sampled in recharge areas = −5.4‰. The sensitivity of the results to variations in end member concentrations within plausible ranges (given observed variability in seawater and fresh groundwater compositions) was examined and found to have minor effect on calculated mixing percentages.

4. Results

4.1. Groundwater salinity and hydrochemistry

Groundwater varies in salinity within the Western Port Basin both laterally and vertically, ranging from fresh (EC of 0.395 mS/cm) to marine-like or slightly above (56.1 mS/cm). Saline water is generally found close to the coastline, consistent with a marine source (Fig. 3). Salinities are also generally greater at shallow depths compared to deeper levels, suggesting a predominantly 'top down' mechanism of saline water emplacement, rather than the typical horizontal or upwards

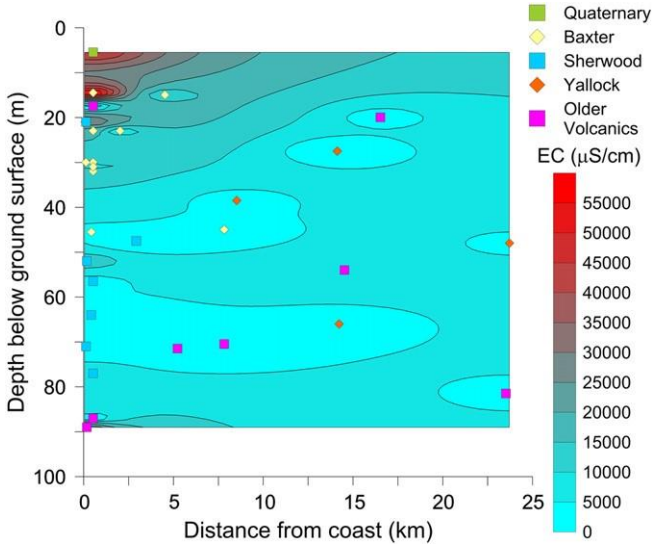

Fig. 3. Distribution of groundwater salinity with distance from coastline and well depth in the Western Port Basin.

pathways associated with 'classic' saline intrusion (Fig. 3). Fig. 4 is a profile along the coast of Western Port showing in detail the distribution of groundwater salinity at different depths and locations, along with the stable isotope ($\delta^{18}O$) and radiocarbon (as pMC) results for each sample.

Groundwater generally is fresher in the east of the basin; this can be explained by proximity and connection to the Heath Hill Fault, a major recharge source (Fig. 1; Currell et al., 2013). On the Western side of the Basin, groundwater salinities near the coastline are higher, with electrical conductivities between 3 and 56.1 mS/cm. Saline water with salinities at or approaching seawater, exists at intermediate depths (25 to 80 m) in the Warneet area (Fig. 4 Sites 1 & 2), and at shallow depths (b15 m) at Tooradin (Fig. 4, site 6). Previously, the Warneet area has been hypothesized as a zone of connate water (Carrillo-Rivera, 1975) or active saline intrusion (Lakey and Tickell, 1980). The coast near Tooradin has also been labeled as an area of potential saline intrusion (Cheng, 1998).

Two distinct vertical profiles of groundwater salinity are observed at different points around the coastline:

- Profile 1 consists of saline water (up to 55.7 mS/cm) in the shallow geology, overlying fresh water (down to 3 mS/cm), in deeper units. Examples of this profile are the nested wells at 'Site 6' (Tooradin) on Fig. 4, and the pore water salinity profile recorded during drilling of a monitoring well nearby (Fig. 5).
- Profile 2 consists of saline water (up to 56.1 mS/cm) in deeper geological units (including the Sherwood and Older Volcanics), that is in some cases overlain by fresher water in the shallower units, for example the locality marked 'Site 2' on Fig. 4.

The hydrochemical facies of the groundwater is shown in Fig. 6 and major ions are reported in Table 2. The majority of groundwater is Na–Cl type, and this is true across the bulk of samples in all salinity ranges (fresh, brackish and saline) and major geological units (Quaternary, Baxter, Sherwood and Older Volcanics). In combination with Cl/Br ratios that are all within typical ranges for marine water (range: 613 to 1070, including 621 to 705 in samples with EC N 15 mS/cm), this indicates that solutes are of predominantly marine origin, as is expected for groundwater recharged either by coastal precipitation and/or direct incorporation of marine water. Locally, some relatively higher proportions of Ca and Mg and HCO_3 occur in groundwater from the Older Volcanics and Sherwood (Fig. 6); this is attributed to minor carbonate dissolution.

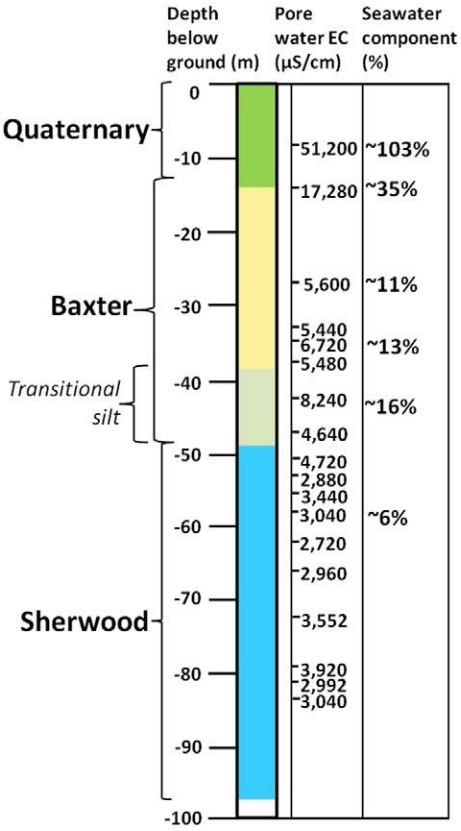

Fig. 5. Porewater salinity measured during drilling of monitoring well 71215 near Tooradin in 1986. Data from Victorian Water Measurement Information System (DELWP Victoria, 2015).

Further detail on the hydrochemical characteristics of groundwater and processes impacting the major ion chemistry can be found in Currell et al. (2013) and Lee (2015).

4.2. Isotopic data: tritium, radiocarbon, $\delta^{18}O$ and $\delta^{2}H$

Few samples contained any significant tritium (Table 3). The only samples with detectable levels (e.g. N0.09 TU) are located near the

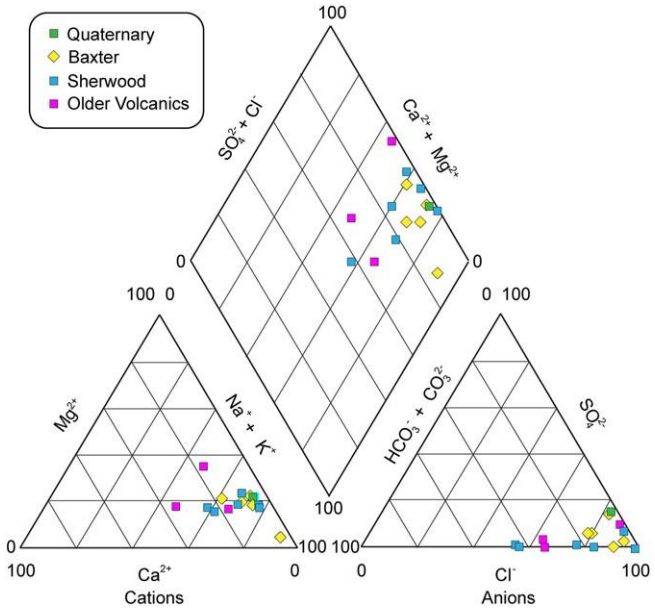

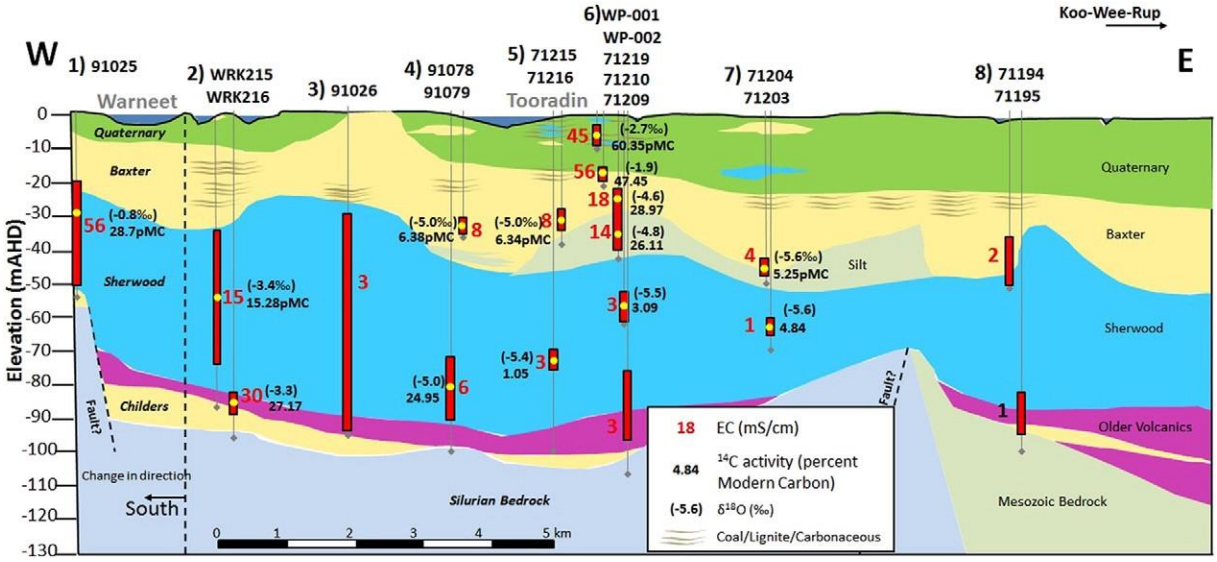

. 4. Transect along the central Western Port coastline showing vertical distribution of salinity (electrical conductivity in mS/cm), radiocarbon activities (percent Modern Carbon as pMC) and stable topes of water ($\delta^{18}O$ and $\delta^{2}H$ in ‰). Monitoring well locations are shown on Fig. 1.

Fig. 6. Piper diagram showing major ion composition of groundwater from the Western Port Basin. Groundwater is dominated by Na and Cl, pointing to a marine source for the majority of solutes.

major faults at the margins of the basin (Fig. 7). This indicates that modern recharge (both rainfall and modern seawater) constitutes a limited component of water in the aquifer system. The current rainfall tritium activities in the Melbourne area are 2.8–3.2 TU (Tadros et al., 2014); hence modern groundwater recharge should approximate this value. Radiocarbon activities in groundwater range from 0.91 to 78.8 pMC (Fig. 7; Table 3). Higher activities occur close to the faults, consistent with these being recharge areas. The other location with relatively high radiocarbon activities is shallow groundwater near Tooradin e.g., wells WP-001 and WP-002, which are saline (ECs of 44.5 and 55.7 mS/cm) with radiocarbon activities of 60.4 and 47.5 pMC, respectively (Fig. 4). Radiocarbon activities at this site, which includes five nested monitoring wells, decrease with depth, as is generally the case in the basin (although two locations near the coastline have the opposite profile —see sites 2 & 4 on Fig 4).

Table 2

The stable isotopes of groundwater are plotted in Fig. 8, ranging from −5.8 to 0.4‰ for $\delta^{18}O$, and −35.6 to −0.8‰ for $\delta^{2}H$. Saline groundwater (EC of N45 mS/cm) has $\delta^{18}O$ values between −2.7 and +0.4, approaching but generally not as high as marine water sampled in Western Port Bay. Fresh groundwater plots in a cluster near the global and local meteoric water lines, shown in Fig. 8, based on data from the Global Network for Isotopes in Precipitation (GNIP) station located approximately

40 km away at Melbourne (weighted mean: $\delta^{18}O$ = −4.99‰, $\delta^{2}H$ = −28.4‰) (IAEA/WMO, 2006). Groundwater samples mostly define a straight mixing pattern between a meteoric end-member and a marine end-member with a composition similar to the local seawater, which was sampled on 4 occasions (Fig. 8). Twocomponent mixing calculations were conducted on this basis, using chloride and oxygen-18 independently (Table 4). Seawater $\delta^{18}O$ and Cl end-members are based on the average observed seawater composition (mean $\delta^{18}O$ of 1.0 and Cl of 521.2 mmol/L, respectively), which is slightly enriched in water isotopes relative to standard marine water. This is attributed to an evaporation effect, given the wide, shallow morphology of Western Port Bay. The meteoric water end-member used in mixing calculations is based on the observed average $\delta^{18}O$ values of fresh groundwater ($\delta^{18}O$ of −5.4‰), which have stable isotopic values slightly depleted relative to weighted mean Melbourne rainfall, towards the winter rainfall weighted average (e.g. $\delta^{18}O$ = −5.9‰). This is consistent with strong seasonality in groundwater recharge and/or recharge during cooler periods in the geological past (Edmunds, 2005; Jasechko et al., 2014; Jasechko et al., 2015).

The proportions of marine water in groundwater estimated using water isotopes (range: 0 to 85.63%) were generally lower than those calculated using chloride (range: 1.0 to 113.7%), particularly in the saline groundwater (Table 2). The chloride values are sensitive to concentration by transpiration, unlike $\delta^{18}O$, which are more sensitive to evaporation but otherwise preserve the composition of the original source water mixtures conservatively (Clark and Fritz, 1997). The relative enrichment of Cl compared to $\delta^{18}O$ suggests that solutes in the water derived from fresh/marine water mixing were in some cases further concentrated by a mechanism that does not fractionate stable isotopes, such as transpiration by vegetation (e.g. Fass et al., 2007; Jasechko et al., 2013).

Major ions and stable isotope data from the Western Port Basin. Ion concentrations are in mmol/L.

Site	Sample date	Unit	EC (μS/cm)	pH	Na	Mg	K	Ca	Cl	Br	NO_3	SO_4	HCO_3	Cl/Br (molar)	$\delta^{2}H$ (‰)	$\delta^{18}O$ (‰)
WP-001	15/08/2014	Quaternary	45,400	6.7	364.5	52.05	6.34	12.74	420.9	0.64	0.02	38.1	14.08	658	−16.0	−2.7
WP-002	15/08/2014	Baxter	55,700	6.63	442.1	61.35	5.94	16.29	559.6	0.82	0.05	32.4	8.72	682	−18.1	−1.9
71204	24/04/2014	Baxter	4061	6.7	23.9	0.54	0.21	0.60	31.5	0.05	0.02	1.15	5.42	630	−34.6	−5.6
71216	24/04/2014	Baxter	7860	6.66	55.4	9.47	0.42	7.92	73.0	0.11	0.01	1.01	4.40	664	−29.7	−4.6
91079	17/01/2012	Baxter	8560	6.34	69.48	11.42	0.82	6.76	68.8	0.10	0.01	1.17	3.80	688	−29.0	−5.0
71219	16/01/2012	Baxter	13,350	6.74	120.00	16.47	2.60	7.50	108.7	0.16	0.20	6.61	8.18	679	−27.8	−4.6
63918	18/05/2013	Baxter	3400	6.82	19.8	2.39	0.06	0.63	27.9	0.03	0.04	0.33	1.85	930	−31.7	−5.5
WRK966215	22/04/2014	Sherwood	14,820	6.93	90.2	13.41	0.26	18.15	118.1	0.19	0.03	4.2	3.64	622	−21.0	−3.1
71203	24/04/2014	Sherwood	1355	7.32	9.1	1.32	0.12	1.93	7.7	0.01	0.01	0.01	5.75	770	−35.6	−5.6
71215	07/05/2014	Sherwood	3160	8.15	22.0	3.17	0.13	1.99	20.0	0.03	0.01	0.14	5.86	667	−34.2	−5.6
91078	15/10/2014	Sherwood	5420	8.16	33.6	5.65	0.14	2.37	50.4	0.07	0.00	0.01	-	720	−33.4	−5.3
91025	19/05/2013	Sherwood	56,100	6.92	500.0	57.20	7.21	16.28	592.4	0.84	1.08	56.3	5.16	705	−0.8	0.08
91025	15/10/2014	Sherwood	53,100	6.92	479.9	54.81	9.01	17.28	583.8	0.92	0.04	31.3	-	635	−2.8	0.4
71209	22/04/2014	Older Volcs	1789	7.89	12.2	1.47	0.00	1.56	10.7	0.01	0.01	0.00	5.45	1070	−34.9	−5.8
WRK966216	22/04/2014	Older Volcs	29,700	7.15	163.0	30.53	0.46	60.21	285.8	0.46	0.10	14.6	6.27	621	−26.6	−3.2
63910	18/05/2013	Older Volcs	869	6.6	3.6	1.29	0.08	0.64	5.4	0.01	0.00	0.14	2.79	540	−33.2	−5.5
Seawater																
WPB 1	15/10/2014	Seawater	51,300	–	423.6	49.1	9.4	10.1	509.6	0.78	0.04	27.6	-	653	−1.1	0.6
WPB 2	26/10/2014	Seawater	51,500	–	435.2	50.2	9.5	10.5	520.9	0.80	0.04	27.8	2.02	651	1.2	0.9
WPB 3	09/11/2014	Seawater	52,100	–	454.4	53.2	9.7	10.8	540.3	0.85	0.08	28.9	–	636	3.6	1.3
WPB 4	18/11/2014	Seawater	55,100	–	439.2	51.7	9.4	10.6	513.8	0.83	0.04	28.6	–	619	1.7	1.2

Table 3

Radioisotope data for groundwater samples. The $a^{14}C$ is radiocarbon activity in units of percent modern carbon (pMC).

Site	Unit	Distance to coast (km)	Depth (well midpoint)	Tritium (TU)	$\delta^{13}C$ (‰)	$a_{14}C$ (pMC)	Age (uncorrected)
WP-001	Quaternary	0.5	5.5	0.05	−17.6	60.35	4055
WP-002	Baxter	0.5	14.5	0.05	−18.4	47.45	5990
71204	Baxter	0.4	45.5	–	−17.6	5.25	23,670
71216	Baxter	0.1	30	–	−14	6.34	22,160
91079	Baxter	0.5	31	–	−15.1	6.38	22,110
63918	Baxter	2	23	0.09	−8.1	54.53	4870
71219	Baxter	0.5	23[a]	–	−19.8	28.97	9955
71219	Baxter	0.5	32[a]	–	−19.9	26.11	10,785
WRK966215	Sherwood	0.15	52	–	−12.7	15.28	15,095
71203	Sherwood	0.4	64	–	−18.4	4.84	24,330
71215	Sherwood	0.1	71	–	−17.1	1.05	36,610
91025	Sherwood	0.1	21	0.08	−7.8	28.7	10,030
WRK966216	Older Volcs	0.15	89	–	−13.5	27.17	10,470
63910	Older Volcs	0.5	17.5	0.05	−19.2	70.12	2850

[a] Sampled different depths in the well screen, using low-flow sampling technique verified by down-hole salinity profiling (Lee, 2015).

5. Discussion

5.1. Groundwater age and origins of groundwater salinity

The three most saline groundwater samples (WP-001, WP-002 and 91025), which have salinities resembling sea-water (EC = 45.4; 55.7 and 56.1 mS/cm) have ^{14}C activities of 60.4, 47.5 and 28.7 pMC, at depths of 5.5 m, 14.5 and 21 m, respectively (Fig. 4). The $\delta^{13}C$ values of the two shallower samples are −17.6 and −18.4‰ respectively (Table 3), consistent with the main source of DIC being CO_2 from decay of vegetation (as opposed to marine water). Other lines of evidence, such as the stable isotopes of water, suggest a predominantly marine source of the water, which would be expected to contribute DIC with a $\delta^{13}C$ value of ~0 ‰.

The DIC concentrations (14.1 and 8.7 mmol/L, respectively) are significantly elevated above typical seawater values (~2 to 2.5 mmol/L). On the basis of the observed $\delta^{13}C$ values we propose that the additional DIC is derived from the carbon fixed by mangroves and other salt-tolerant coastal vegetation that has long been native to the region. Miyajima et al. (2009); Maher et al. (2013) and Alongi (2014) showed that coastal mangrove communities contribute substantial DIC (as well as DOC) to water and soils in coastal swamp environments, acting as an effective CO_2 pump from the atmosphere to estuaries through surface and subsurface pathways. Saintilan et al. (2013) measured $\delta^{13}C$ compositions of soils and plant matter in southeast Australian mangrove swamps including Western Port, and found values of ~−27‰ for

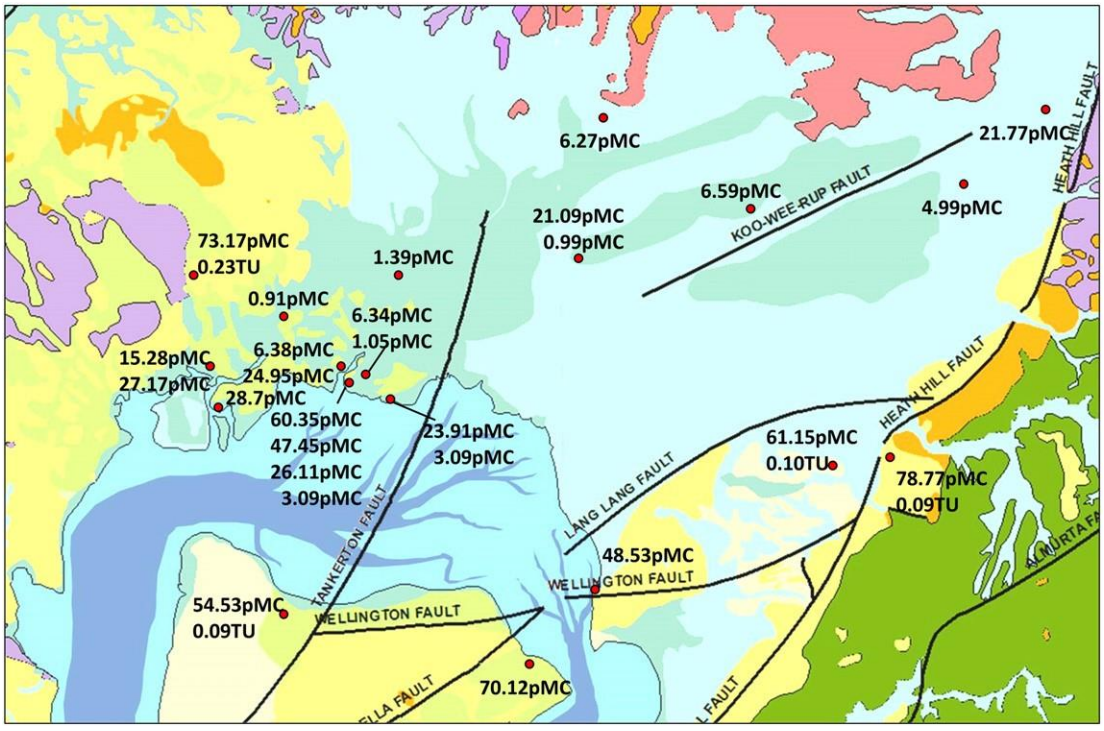

Fig. 7. Map showing groundwater radiocarbon activities (pMC) in groundwater along with tritium concentrations (TU). Labels at nested sites are in order from shallow to deep from top to bottom.

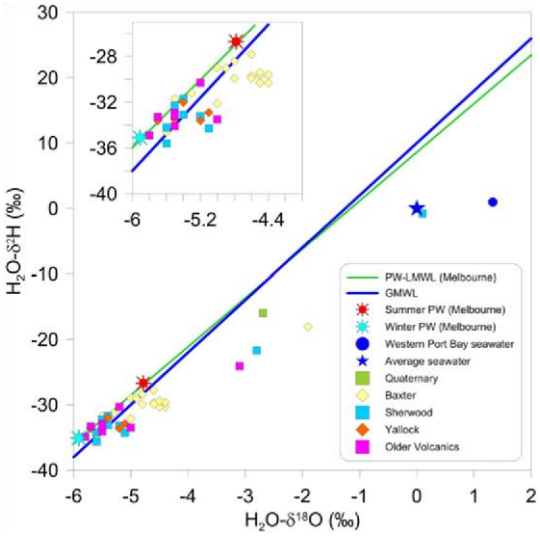

Fig. 8. Stable isotopic compositions of groundwater and sea water samples. Local Meteoric Water Line (LMWL) sourced from IAEA/WMO (2006) and calculated following Hughes and Crawford (2012); average precipitated weighted rainfall for summer (DJF) and Winter (JJA) calculated from the IAEA/WMO (2006) dataset; Global Meteoric Water Line (GMWL) from Craig (1961).

Table 4
Calculated percentages of marine water in groundwater samples, based on two-component mixing calculations using chloride and oxygen-18.

Site	Unit	EC (µS/cm)	Cl (mmol/L)	$\delta_{18}O$ (‰)	%Seawater (from Cl)	%Seawater (from $\delta_{18}O$)
WP-001	Quaternary	45,400	420.92	−2.7	80.75	42.34
WP-002	Baxter	55,700	559.65	−1.9	107.38	54.68
71204	Baxter	4061	31.5	−5.6	6.01	0
71216	Baxter	7860	73.0	−4.6	13.98	12.02
63918	Baxter	3400	27.9	−5.5	5.33	0
71219	Baxter	13,350	108.7	−4.5	20.84	13.58
91079	Baxter	8560	68.8	−4.9	13.17	7.81
WRK966215	Sherwood	14,820	118.1	−3.1	18.57	36.20
71203	Sherwood	1355	7.7	−5.6	11.90	0
71215	Sherwood	3160	20.0	−5.6	19.24	0
91078	Sherwood	5420	50.4	−5.3	13.30	1.12
91025	Sherwood	56,100	592.4	0.08	113.7	85.63
71209	Older Volcs	1789	10.7	−5.8	2.02	0
WRK966216	Older Volcs	29,700	285.8	−3.2	54.82	34.47
63910	Older Volcs	869	5.4	−5.5	1.00	0

mangrove and −15 to −12‰ for seagrasses, the two dominant types of vegetation at Western Port. Using isotope mass balance (equation 3), we estimate approximate proportions of DIC derived from seawater, mangrove and seagrass in these samples. Assuming 2.3 mmol/L of DIC is derived from the original seawater emplaced in the aquifer (with $\delta^{13}C = 0$), the observed $\delta^{13}C$ values can be arrived at if 55 to 85% of the additional DIC is from mangrove and 45 to 15% from seagrass.

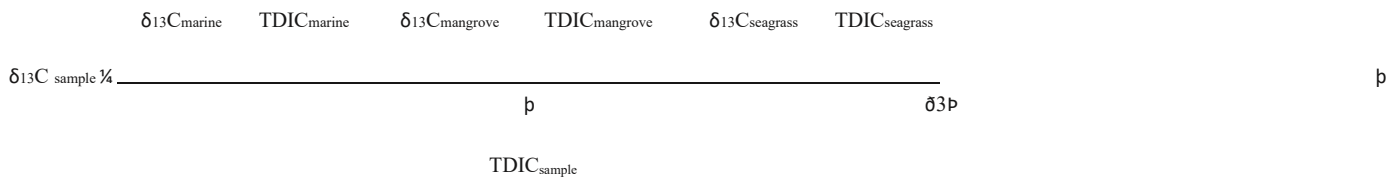

where TDIC = total dissolved inorganic carbon (mmol/L) and the end member $\delta^{13}C$ values for marine water, mangrove and seagrass are 0‰, −27‰ and −13.5‰, respectively (Saintilan et al., 2013).

As is further discussed below, the conceptual model of the origins of groundwater salinity at these locations is that mixing occurred between marine and fresh water inputs in a palaeo-swamp environment during the middle Holocene, with extensive interaction between shallow groundwater and halophyte vegetation. This would be expected to cause modification of the groundwater DIC pool towards vegetation compositions, given the high rates of carbon fixation by this vegetation.

The $\delta^{13}C$ value of sample 91025 is more positive (−7.8‰), which may suggest a larger component of marine water and/or marine carbonate in the groundwater. Carbonate occurs within the Sherwood formation where this well is screened. Again the higher DIC concentration compared to seawater (5.16 mmol/L) indicates significant addition from vegetation and/or mineral dissolution; the $\delta^{13}C$ value implies at least some component is derived from vegetation, in addition to aquifer carbonate (although less than in WP-001 and WP-002).

Ranges of corrected and uncorrected groundwater ages estimated for the three saline samples, along with another slightly less saline sample at Warneet (WRK966216, EC = 29.7 mS/cm) are shown in Table 5. The range of age estimates encompasses the minimum (corrected) and maximum (uncorrected) ages, using a range of assumptions about sources of DIC in the water. Consistent with the above discussion, samples WP-001 and WP002 were modeled to obtain the majority of carbon from vegetation, while sample 91025 is assumed to have a larger component of DIC derived from carbonate minerals. We acknowledge that there is significant uncertainty in the contribution of DIC sources associated with various possible combinations of sources and end-member $\delta^{13}C$ values.

Notwithstanding the uncertainty, the estimated age ranges of these saline samples (uncorrected and corrected) are all within the Holocene, and are consistent with emplacement of marine water in the aquifer during the mid-Holocene high sea stand, which occurred sometime between ~2 and 8 kyr BP (Sloss et al., 2007). This is in contrast to past speculation that saline water found at Warneet and Tooradin is due to modern seawater intrusion caused by over-extraction of groundwater in the Koo Wee Rup region (Lakey and Tickell, 1980) and/or connate water emplaced at the time of sediment deposition (Carrillo-Rivera, 1975). The lack of detectable tritium also supports the idea that although these samples resemble seawater in salinity and ion chemistry, they are not modern.

This emplacement mechanism is consistent with the geomorphological evidence around the coastline. The higher sea-level in the mid-Holocene is evident in the occurrence of marine deposits, beach ridges and stranded cliff-lines to a distance of 1 to 1.5 km inland around Western Port (Marsden and Mallett, 1975). At this time, extensive parts of the present coastline were inundated, and fringed by wide coastal swampland, including salt marsh and mangrove (Spencer-Jones et al., 1975; Marsden and Mallett, 1975). The interaction of saline water with vegetation in this swampland during gradual downwards infiltration into the clay-rich sediments, may explain why the $\delta^{13}C$ values have vegetation signal rather than marine water signatures, as well as the additional salinization by transpiration suggested by the stable isotope and chloride data (Section 4.2).

An alternate explanation for the observed hydrochemical and isotope compositions could be that the saline water at Tooradin and Warneet represents the leading edge of a modern seawater intrusion front, with relatively lower radio-isotope activities than in the plume centre (which would be expected to have isotopic compositions approximating modern seawater, accounting for reservoir effects). This model is less consistent with the vertical salinity profile observed at Tooradin, where saline water occurs at shallow levels (5 to 15 m below surface), underlain by deeper fresh water

Table 5
Uncorrected and corrected groundwater ages for saline groundwater at the coastline of Western Port. Uncorrected ages are considered the maximum age, while corrected ages listed are the minimum age determined using 2 or more models and assumptions regarding sources of dissolved inorganic carbon using the NETPATH code(Plummer et al., 1994; Han and Plummer, 2013). For raw data and full list of radiocarbon results, see Tables 2 & 3.

Sample no.	Salinity (EC, mS/cm)	$\delta_{18}O$ (‰)	Radiocarbon activity (pMC)	$\delta_{13}C_{DIC}$ (‰)	Age (uncorrected)	Age (corrected, min)
WPB-001	45.4	−2.7	60.4	−17.6	4055	2000
WPB-002	55.7	−1.9	47.5	−18.4	5990	4400
91025	56.1	0.4	28.7	−7.8	10,030	550
WRK966216	29.7	−3.2	27.2	−13.5	10,470	6300

— the inverse of a classic salt water 'wedge'. It is also less consistent with the fact that the Quaternary clays, where the saline water is found, have low permeability and are generally not accessed for groundwater extraction. Significant water level declines in response to pumping occur in the underlying Baxter and Sherwood Formations, rather than the clays. Thus, salt water would be expected to emerge at deeper levels than is observed if the saline water represented a modern seawater intrusion front. Finally, modern seawater intrusion is less consistent with the observed $\delta^{13}C$ values, which would be expected to retain marine-like ratios, as sub-surface intrusion would leave minimal opportunity for interaction with vegetation.

Trapping of marine water emplaced during the middle Holocene from surface inundation could be facilitated by the Quaternary clays, allowing an inherently unstable density configuration (saline water overlying freshwater) to remain intact since that time. Previous modeling of vertical salinization processes indicates that where clays are of low enough permeability, downward propagation of saline water is dominated by diffusion, which occurs at slow rates. This can protect underlying freshwater for up to thousands of years (Groen et al., 2000; Post and Kooi, 2003). Some flushing and downward propagation of the trapped marine water (by advection or diffusion) appears to have occurred, as indicated by 1) the slightly fresher salinity in the shallowest sample (at 5.5 m) compared to the sample immediately below (at 14.5 m); 2) stable isotope compositions in the shallow water that are depleted relative to marine water, following a mixing line with meteoric water; this implies a contribution from a rainfall-derived fresh end-member (Fig. 7); 3) intermediate salinities (13.5 mS/cm), radiocarbon activities (26.1 pMC) and stable isotopic values ($\delta^{18}O$ of −4.5‰) found immediately below the saline samples in the upper Baxter formation at 20 m depth (sample 71219 — Fig. 4). These lines of evidence are all consistent with slow downwards salinization from a marine water source emplaced above deeper fresh water.

5.2. Conceptual models of saline water emplacement

Conceptual models to explain the emplacement of saline water in the Western Port aquifer, and the resulting vertical salinity profiles and isotopic data at Tooradin and Warneet are shown in Figs. 9 & 10, respectively. The vertical profile of groundwater salinities, radiocarbon activities and stable isotopes – all decreasing with depth – at Tooradin (Fig. 4, site 6), is essentially an inverted saline wedge, with all isotopic indicators consistent with saline water of marine origin emplaced by surface inundation in the mid-Holocene, mixing gradually with underlying fresh groundwater of late Pleistocene age. However, two component mixing calculations in the saline shallow samples using stable isotopes of water suggest only ~50% marine water, mixing with a fresh end-member (such as pre-existing fresh ground or surface water). The additional concentration of solutes required to reach observed Cl concentrations must have occurred due to a mechanism which does not fractionate stable isotopes, hence samples remain on the mixing line between fresh and meteoric water (Fig. 8). On the basis of the predominantly marine-like ion ratios – molar Cl/Br ratios are between 621 and 705 in samples with EC ≥ 15 mS/cm (Table 2) — the mechanism of solute concentration is proposed to be transpiration and solute exclusion by halophytic vegetation, rather than mineral dissolution. This is consistent with the observed $\delta^{13}C$ values, which indicate significant interaction with decaying vegetation matter in the soil zone during recharge. If mineral dissolution (such as halite) were responsible for the increased salinity and Cl values, then elevated Cl/Br ratios would be expected (e.g. Davis et al., 1998).

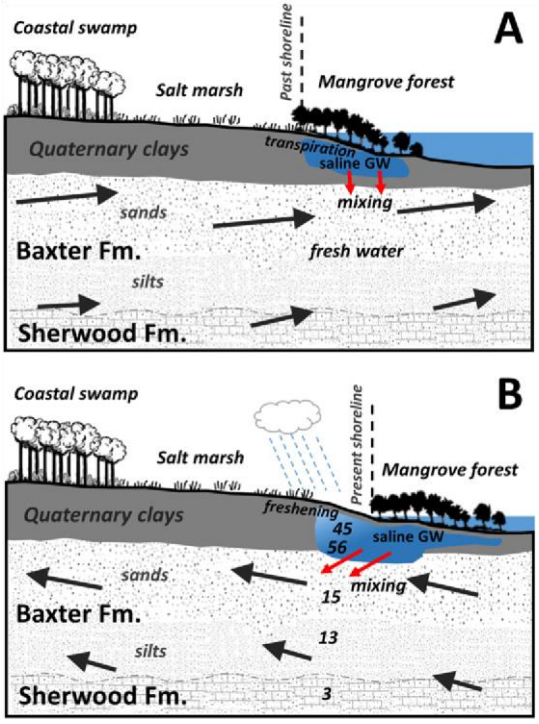

Fig. 9. Conceptual model showing emplacement of saline water in the upper Western Port basin during mid-Holocene high sea-stand, and subsequent downward vertical mixing at the Tooradin site. Numbers in black are groundwater EC in mS/cm; arrows indicate predominant groundwater flow direction in the pre-development and post-development Western Port basin. Groundwater flow directions are now predominantly towards the in-land pumping area (see Section 5.3).

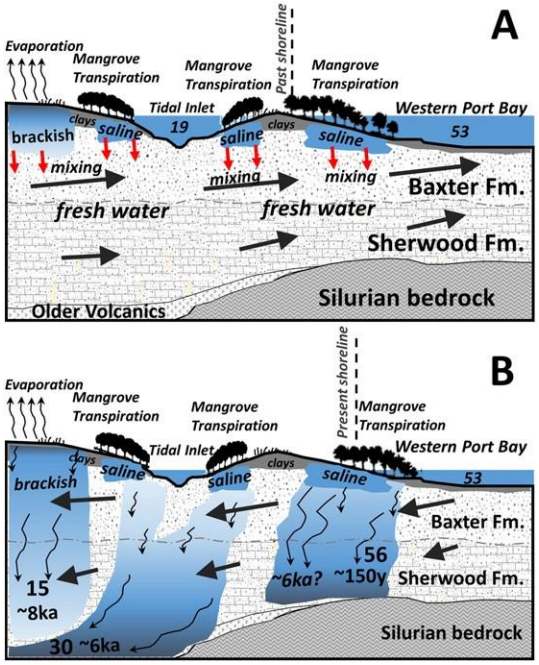

Fig. 10. Conceptual model showing proposed mechanism of saline water emplacement at Warneet (sites 1 & 2 of Fig. 4). Saline water (bold numbers are EC in mS/cm) has propagated deeper into the aquifer at this location than at Tooradin, due to a lack of confining clays. Arrows in black indicate predominant groundwater flow direction (A) prior to and (B) after development of the aquifer for irrigation.

The palaeo-environment of the Western Port coastline was a swampland, based on analysis of a range of Quaternary sedimentary and geomorphological evidence (Marsden et al., 1979). Periodic inundation of this environment with saline water during the mid-Holocene high sea-stand, along with input of meteoric water from rainfall and surface water would allow a) mixing between fresh and marine water, producing the observed stable isotopic compositions; b) concentration of solutes by transpiration, producing the observed salinities, during gradual infiltration into the shallow low-permeability Quaternary deposits; c) modification of the DIC pool as CO_2fixed by mangroves and other vegetation is incorporated into the shallow infiltrating groundwater (e.g. Fig. 9). As noted earlier, some subsequent infiltration of modern meteoric water may be responsible for the additional freshening and isotopic shift observed in the shallowest sample (WP-001). As is discussed further below (Section 5.3), groundwater pumping in modern times may also be contributing to gradual downwards leakage of the saline water.

In contrast to the profile observed at Tooradin, saline water is found at deeper levels at Warneet, where Quaternary clay deposits are absent (e.g. Fig. 10, Fig. 4). This implies the saline water from the same period of high sea level may have been able to propagate downwards more rapidly into the underlying aquifer units, due to the absence of a clay layer. For example, one sample near Warneet, from a relatively deep position in the aquifer (80 m below surface) has an EC of 29 mS/cm and an estimated groundwater age between 6300 and 10,470 years BP (incorporating the minimum corrected and uncorrected ages). This is slightly older than the shallow marine-like water at Tooradin (Table 3). This water also has a more depleted stable isotope ratio ($\delta^{18}O$ of −3.2‰). The fresher salinity and older radiocarbon age in this water are consistent with mixing between a mid-Holocene saline component and an older existing fresh groundwater component in the aquifer, encountered (for example) during rapid downwards propagation of the saline water from above (Fig. 10).

At site 91025, which contains water with marine-like salinity and the most marine-like stable isotope compositions of the dataset (e.g., $\delta^{18}O$ of 0.1‰), the lower radiocarbon activity (28.7 pMC) accompanied by enriched $\delta^{13}C$ (−7.8‰) implies significant interaction with carbonate minerals. This is consistent with the marine, carbonate-rich lithology of the Sherwood Formation being present at shallower depths at this locality, again with an absence of the confining Quaternary clay. The absence of the clay can here again explain why saline water is found relatively deeper (~25 m) at Warneet compared to Tooradin (~5 to 15 m). The correction of

the radiocarbon age at this locality is more uncertain than other samples due to likely significant input from the aquifer matrix. The difference between minimum and maximum ages using NETPATH is thus relatively large, depending on assumptions made about the origins of water and DIC (Table 5). In the most extreme case, the corrected age approximates modern water (550 years — which could be essentially modern accounting for reservoir effects), meaning recent saline intrusion at this locality can't be ruled out completely. Still, if the true groundwater age is somewhere between the maximum (uncorrected) age of 10.03 kyr BP and the minimum corrected age of 0.55 kyr BP, this would be consistent with emplacement of the saline water during the mid-Holocene, contemporaneous with that observed at Tooradin.

5.3. Water management implications

In recent years (e.g. since the 1960s) there has been sustained pumping of fresh groundwater for irrigation in the Western Port Basin in the confined aquifers of the Western Port Group and Older Volcanics (Southern Rural Water, 2010). This is likely to be enhancing the rate of downwards and horizontal propagation of the trapped shallow saline water into the deeper aquifer system, depending on the thickness and permeability of the shallow confining layers. It is not known at present what the impact of extensive groundwater development of the confined aquifer system further inland of the coast since the mid-20th Century may have had on the stability of the salinity configuration at Tooradin, with dense saline water overlying less dense fresh water. Pumping causes seasonal drawdowns of up to ~4 m in some areas within the confined Baxter, Sherwood and Older Volcanics aquifers to the north of the coastline.

Fig. 11 shows potentiometric head contours in the confined aquifer during February, 2014 during the peak period of seasonal groundwater extraction. Areas with the head contour below sea level are shown in red. It is in these areas that the groundwater is most vulnerable to salinsation, whether by lateral seawater intrusion or vertical leakage of the trapped marine water. The seasonal drawdown creates hydraulic gradients which are conducive to either mechanism, but the former is considered more important in the Warneet area due to proximity to the deep offshore tidal channel, whereas the latter (vertical leakage) is considered more of a risk at Tooradin, where trapped saline water in the Quaternary clays lies immediately above the confined aquifers. Here, the rates of leakage are only constrained by the permeability of the geology. During non-pumping periods, potentiometric head levels typically recover back above sea-level, meaning the opportunity for such leakage is limited to certain parts of the year when pumping is most intensive (Southern Rural Water, 2010).

Monitoring of groundwater salinities over the past 2–3 decades reveals little evidence of a long-term increase in salinity of the groundwater in the confined aquifers, including at coastal monitoring bores near Tooradin and Warneet. This indicates limited leakage of saline water into the freshwater aquifers to date (Southern Rural Water, 2010). Over a longer timeframe, the pumping may be inducing gradual downwards leakage of a saline plume through the Quaternary sediments towards the deeper freshwater aquifers (e.g. Fig. 9). It is notable that saline water appears to have reached the upper Baxter formation sediments at site WP-002 (Fig. 4; Fig. 9); this may be a response to large drawdowns in this aquifer over recent decades. Groundwater in the underlying Sherwood Formation (Sample 71210) still remains relatively fresh at Tooradin (b2 g/L TDS) apparently protected from downward mixing, possibly due to silt at the base of the Baxter Formation (Fig. 4).

The insights gained from our isotopic data place a new constraint on the age and origin of saline water, indicating that much of the salinity in the system is relatively old (compared to previous thinking) and hence there may be greater level of inertia and buffering capacity against salinisation than previously thought (cf. Lakey and Tickell, 1980). However, regardless of whether saline water represents that which was emplaced in the mid-Holocene, or modern seawater from 'classic' horizontal seawater intrusion, management of groundwater for long term sustainability should focus on preventing large inland and downwards hydraulic gradients developing in response to pumping, and/or long-term declines in the water levels of the water supply aquifers (e.g., without seasonal recovery). This is the only strategy that can effectively protect against migration of saline

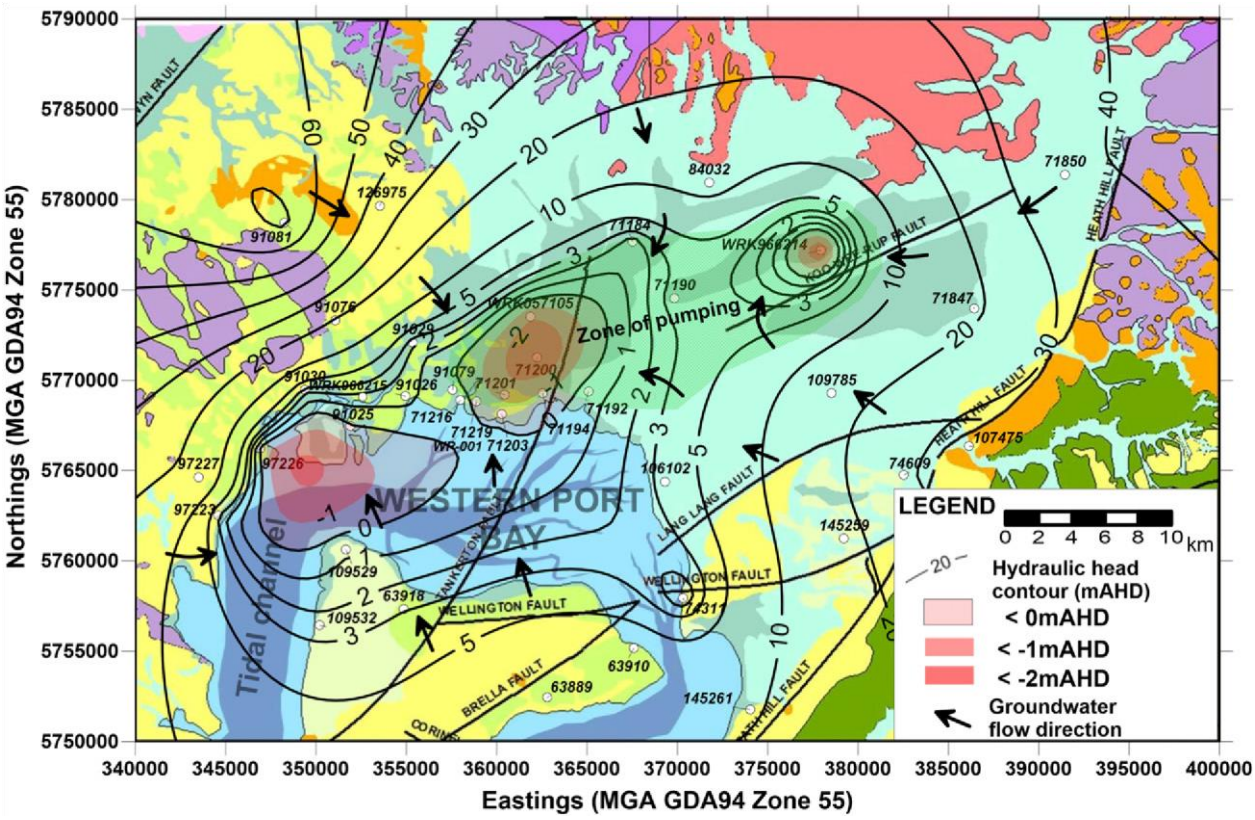

Fig. 11. Map of potentiometric head levels in the confined Western Port Group aquifer, highlighting areas most vulnerable to saline intrusion through horizontal ingress and/or vertical leakage of saline water trapped in the Quaternary clays. For key to geological units, refer to Fig. 1.

water, irrespective of its age and origin, or the rate at which intrusion (whether by downwards leakage or horizontal movement) is limited by the geological properties.

The same phenomenon we have observed at Western Port – the occurrence of trapped palaeo-seawater in shallow low permeability sediments – also appears to occur in other low-lying coastal aquifers that were inundated by seawater during the mid-Holocene (e.g. Vaeret et al., 2012; Cary et al., 2015). We propose that dating of saline water in coastal aquifers using radiocarbon, tritium and other appropriate techniques, along with a detailed examination of vertical profiles of salinity and stable isotopes, are important steps required to distinguish typical seawater intrusion modes from palaeo-marine water emplacement. Future management of these systems can then model and account for the timescales of salinisation and freshening processes more realistically.

6. Conclusions

A range of isotopic-geochemical indicators ($\delta^{18}O$, $\delta^{2}H$, major ions, radiocarbon, $\delta^{13}C$ and tritium) were analyzed in groundwater along the coastline of the Western Port Basin, in order to investigate the origins of groundwater salinity in the aquifer system. It was determined that in one area containing an 'inverted' salinity profile, saline shallow groundwater was emplaced by surface inundation in the midHolocene, and has been trapped within Quaternary clays above fresh groundwater of meteoric origin. In other areas, saline groundwater, probably of the same age and origin, has reached deeper levels in the aquifer and now underlies fresher groundwater, as is typically expected in coastal systems.

These results indicate that groundwater near the coastline has in places yet to equilibrate with changes in sea-level over the last ~20 kyr. A difference in the estimated mixing ratios of meteoric and marine water was determined when using chloride and stable isotope compositions independently. This suggests that groundwater salinization has also to some degree occurred due to transpiration and solute exclusion, by halophytic coastal vegetation, in addition to emplacement of marine water. Vegetation-like $\delta^{13}C$ signatures in saline shallow groundwater indicate extensive interaction between mangroves and possibly sea-grasses in the paleo-swampland of Western Port during the Middle-Holocene. These data further support the hypothesis of saline water emplacement by surface inundation, rather than lateral sub-surface intrusion.

Based on the observed vertical profiles of salinity, it would be expected that downwards propagation of saline water into the underlying fresh aquifers should be occurring. The fact that this has not occurred to a major degree (based on monitored salinity levels in the deeper aquifers) indicates the upper confining layers are relatively low in permeability, and salinization is unlikely to happen rapidly. However, in order to limit the migration of trapped saline bodies of water in the basin to areas of fresh groundwater in the future, pumping rates in the confined aquifers should be limited so that large vertical (and horizontal) gradients do not develop.

These findings are of major significance for environmental and water management of coastal groundwater systems, and for the scientific community. Our study indicates that in areas of low-lying coastline that are b2 m above present sea level, there is the potential for saline water to be present in shallow aquifers due to surface inundation by marine water in the mid-Holocene, and subsequent trapping. Whether such water is preserved in a given environment depends predominantly

on the makeup of the geological profile, and in particular whether low permeability horizons exist. This may lead to a re-interpretation in some settings of the origins of saline groundwater — for example showing that long-term geological processes may be more important than modern day saline intrusion. While downwards leakage of trapped saline water and lateral intrusion are fundamentally different processes, groundwater management strategies for both cases should still focus on limiting negative hydraulic gradients between saline and fresh water bodies.

7. Acknowledgements

UNESCO IGCP-618 project (Paleoclimate information obtained from past-recharged groundwater) and the G@GPS network are acknowledged for financial support. We thank three anonymous peerreviewers for their comments which helped to improve the manuscript, and the editor of Science of the Total Environment, Prof. Damià Barceló.

References

Alongi, D.M., 2014. Carbon cycling and storage in mangrove forests. Annu. Rev. Mar. Sci. 6, 195–219.

Baker, D.J., Lakey, R.C., Evans, R.S., 1986. Management options for Westernport groundwater basin, Victoria. Proceedings of the Australian Water Resources Council Conference: Groundwater Systems Under Stress, pp. 101–110.

Carrillo-Rivera, J.J., 1975. Hydrogeology of Western Port. Geological Survey of Victoria Report (Victoria) 1975/1. Mines Department, Victoria 32 pp.

Cartwright, I., Weaver, T., Cendón, D.I., Swane, I., 2010. Environmental isotopes as indicators of inter-aquifer mixing, Wimmera region, Murray Basin, Southeast Australia. Chem. Geol. 277, 214–226.

Cary, L., Petelet-Giraud, E., Bertrand, G., Kloppmann, W., Aquilina, L., Martins, V., Hirata, R., Montenegro, S.M.G.L., Pauwels, H., Chatton, E., et al., 2015. Origins and processes of groundwater salinization in the urban coastal aquifers of Recife (Pernambuco, Brazil): a multi-isotope approach. Sci. Total Environ. 530-531, 411–429.

Cendón, D.I., Hankin, S.I., Williams, J.P., Van der Ley, M., Peterson, M., Hughes, C.E., Meredith, K., Graham, I.T., Hollins, S.E., Levchenko, V., Chisari, R., 2014. Groundwater residence time in a dissected and weathered sandstone plateau: Kulnura–Mangrove Mountain aquifer, NSW. Australia: Aust. J Earth Sci. 61, 475–499.

Cheng, X., 1998. Impact of Groundwater Abstraction on Groundwater Flow and Solute Transport, Western Port Basin, Victoria. University of Melbourne, MSc Thesis 358 pp.

Clark, I., Fritz, P., 1997. Environmental Isotopes in Hydrogeology. CRC Press 328 pp.

Craig, H., 1961. Isotopic variations in meteoric waters. Science 133, 1702–1703.

Currell, M., Cendón, D.I., Cheng, X., 2013. Analysis of environmental isotopes in groundwater to understand the response of a vulnerable coastal aquifer to pumping: Western Port Basin, south-eastern Australia. Hydrogeol. J. 21, 1413–1427.

Currell, M.J., Dahlhaus, P., Ii, H., 2014. Stable isotopes as indicators of water and salinity sources in a southeast Australian coastal wetland: identifying relict marine water, and implications for future change. Hydrogeol. J. 1-14.

Davis, S.N., Whittemore, D.O., Fabryka-Martin, J., 1998. Uses of chloride/bromide ratios in studies of potable water. Ground Wat. 36, 328–350.

Department of Environment, Land, Water and Planning Victoria, 2015i. Victorian water measurement information system (WMIS). available at: http://data.water.vic.gov.au/monitoring.htm (accessed March 2013 to October 2015).

Edmunds, W.M., 2005. Groundwater as an archive of climate and environmental change. Isotopes in the Water Cycle: Past, Present and Future of a Developing Science, pp. 341–352.

Fass, T., Cook, P.G., Stieglitz, T., Herczeg, A.L., 2007. Development of saline ground water through transpiration of sea water. Ground Wat. 45, 703–710.

Ferguson, G., Gleeson, T., 2012. Vulnerability of coastal aquifers to groundwater use and climate change. Nat. Clim. Chang. 2, 342–345.

Fink, D., Hotchkis, M., Hua, Q., Jacobsen, G., Smith, A.M., Zoppi, U., Child, D., Mifsud, C., van der Gaast, H., Williams, A., Williams, M., 2004. The ANTARES AMS facility at ANSTO. Nucl. Instrum. Meth. B. 223-224, 109–115.

Giambastiani, B.M.S., Colombani, N., Fidelibus, M.D., Severi, P., Mastrocicco, M., 2012. Groundwater hypersalinization in a lowland coastal aquifer (Po river plain, Italy). Proceedings of the 22nd Salt Water Intrusion Meeting, pp. 82–85.

Groen, J., Velstra, J., Meesters, A.G.C.A., 2000. Salinization processes in paleowaters in coastal sediments of Suriname: evidence from $\delta^{37}Cl$ analysis and diffusion modelling. J. Hydrol. 234, 1–20.

Han, L.-F., Plummer, L.N., 2013. Revision of Fontes & Garnier's model for the initial 14C content of dissolved inorganic carbon used in groundwater dating. Chem. Geol. 351, 105–114.

Hughes, C.E., Crawford, J., 2012. A new precipitation weighted method for determining the meteoric water line for hydrological applications demonstrated using Australian and global GNIP data. J. Hydrol. 464, 344–351.

IAEA/WMO, 2006. Global Network of Isotopes in Precipitation. The GNIP Database. (http://www.iaea.org/water).

Jasechko, S., Sharp, Z.D., Gibson, J.J., Birks, S.J., Yi, Y., Fawcett, P.J., 2013. Terrestrial water fluxes dominated by transpiration. Nature 496, 347–351.

Jasechko, S., Birks, S.J., Gleeson, T., Wada, Y., Fawcett, P.J., Sharp, Z.D., McDonnell, J.J., Welker, J.M., 2014. The pronounced seasonality of global groundwater recharge. Water Resour. Res. Doi: http://dx.doi.org/10.1002/2014WR015809.

Jasechko, S., Lechler, A., Pausata, F.S.R., Fawcett, P.J., Gleeson, T., Cendón, D.I., Galewsky, J., LeGrande, A.N., Risi, C., Sharp, Z.D., Welker, J.M., Werner, M., Yoshimura, K., 2015. Glacial–interglacial shifts in global and regional precipitation $\delta^{18}O$. Clim. Past 11, 831–872.

Jenkin, J.J., 1962. The geology and hydrogeology of the Western Port area. Geological Survey of Victoria Underground Water Investigation Report No. 5, Mines Department, Victoria 81pp.

Kafri, U., Yechieli, Y., 2010. Groundwater Base Level Changes and Adjoining Hydrological Systems. Springer 171 pp.

Kooi, H., Groen, J., Leijnse, A., 2000. Modes of seawater intrusion during transgressions. Water Resour. Res. 36, 317–320.

Kooi, H., Groen, J., 2003. Geological processes and the management of groundwater resources in coastal areas. Neth. J. Geosci. 82, 31–40.

Lakey, R., Tickell, S.J., 1980. Effects of channel dredging in the Tyabb area on Western Port Basin groundwater. Geological Survey of Victoria Report 58, Mines Department, Victoria 40 pp.

Lee, S., 2015. Investigating the origin and dynamics of salinity in a confined aquifer system in southeast Australia (Western Port Basin) (Master of Engineering Thesis) RMIT University Available at: https://researchbank.rmit.edu.au/view/rmit:161422.

Lewis, S.E., Sloss, C.R., Murray-Wallace, C.V., Woodroffe, C.D., Smithers, S.G., 2013. Postglacial seal-level changes around the Australian margin: a review. Quaternary Sci. Rev. 74, 115–138.

Maher, D.T., Santos, I.R., Golsby-Smith, L., Gleeson, J., Eyre, B.D., 2013. Groundwaterderived dissolved inorganic and organic carbon exports from a mangrove tidal creek: the missing mangrove carbon sink? Limnol. Oceanogr. 58, 475–488.

Marsden, M.A.H., Mallett, C.W., 1975. Quaternary evolution, morphology and sediment distribution, Westernport Bay, Victoria. Proc. R. Soc. Vic. 87, 107–138.

Marsden, M.A.H., Mallett, C.W., Donaldson, A.K., 1979. Geological and physical setting, sediments and environments, Western Port, Victoria. Mar. Geol. 30, 11–46.

Miyajima, T., Tsuboi, Y., Tanaka, Y., Koike, I., 2009. Export of inorganic carbon from two Southeast Asian mangrove forests to adjacent estuaries as estimated by the stable isotope composition of dissolved inorganic carbon. J. Geophys. Res. 114, G01024.

Morgenstern, U., Taylor, C.B., 2009. Ultra low-level tritium measurement using electrolytic enrichment and LSC. Isot. Environ. Healt. S. 45, 96–117.

Morrissey, S.K., Clark, J.F., Bennett, M., Richardson, E., Stute, M., 2010. Groundwater reorganization in the Floridan aquifer following Holocene sea-level rise. Nat. Geosci. 3, 683–687.

Plummer, L.N., Prestemon, E.C., Parkhurst, D.L., 1994. An interactive code (NETPATH) for modeling NET geochemical reactions along a flow PATH — Version 2.0: U.S. Geological Survey Water-Resources Investigations Report 94-4169 130pp.

Post, V.E.A., Kooi, H., 2003. Rates of salinization by free convection in high-permeability sediments: insights from numerical modelling and application to the Dutch coastal area. Hydrogeol. J. 11, 549–559.

Post, V.E.A., Groen, J., Kooi, H., Person, M., Ge, S., Edmunds, W.M., 2013. Offshore fresh groundwater reserves as a global phenomenon. Nature 501, 71–78.

Saintilan, N., Rogers, K., Mazumder, D., Woodroffe, C., 2013. Allochthonous and autochthonous contributions to carbon accumulation and carbon store in southeastern Australian coastal wetlands. Estuar. Coast Shelf S. 128, 84–92.

Sloss, C.R., Murray-Wallace, C.V., Jones, B.G., 2007. Holocene sea-level change on the southeast coast of Australia: a review. The Holocene 17, 999–1014.

Southern Rural Water, 2010. Groundwater Management Plan, Koo Wee Rup Water Supply Protection Area 25 pp.

Spencer-Jones, D., Marsden, M.A.H., Barton, C.M., Carrillo-Rivera, J.J., 1975. Geology of the Western Port Sunkland. Proc. R. Soc. Vic. 87, 43–68.

Stuiver, M., Polach, A., 1977. Reporting of ^{14}C data. Radiocarbon 19, 355–363.

Tadros, C.V., Hughes, C.E., Crawford, J., Hollins, S.E., Chisari, R., 2014. Tritium in Australian precipitation: a 50 year record. J. Hydrol. 513, 262–273.

Thompson, B.R., 1974. The geology and hydrogeology of the Western Port sunklands. Mines Department, Victoria 78pp.

Vaeret, L., Jeijnse, A., Cuamba, F., Haldorsen, S., 2012. Holocene dynamics of the salt-fresh groundwater interface under a sand island, Inhaca. Mozambique. Quatern. Int. 257, 74–82.

Werner, A.D., Bakker, M., Post, V.E.A., Vandenbohede, A., Lu, C., Ataie-Ashtiani, B., Simmons, C.T., Barry, D.A., 2013. Seawater intrusion processes, investigation and management: recent advances and future challenges. Adv. Water Resour. 51, 3–26.